Multiphase semiclassical approximation of the one-dimensional harmonic crystal: I. The periodic case

Laurent Gosse

Multiphase semiclassical approximation of the one-dimensional harmonic crystal

‡

Laurent Gosse

Istituto per le Applicazioni del Calcolo (sezione di Bari), via G. Amendola, 122/D, 70126 BARI, Italy

E-mail: l.gosse@ba.iac.cnr.it

AMS classification scheme numbers: Primary 81Q05,81Q20; Secondary 35L65, 65M06

Abstract. One-dimensional electronic conduction is investigated in a special case usually referred to as the harmonic crystal, meaning essentially that atoms are assumed to move like coupled harmonic oscillators within the Born-Oppenheimer approximation. We recall their dispersion relation and derive a WKB system approximately satisfied by any electron's wave-function inside a given energy band. This is then numerically solved according to the theory of K-branch solutions. Numerical results are presented in case atoms move with one- or two-modes vibrations; at last, we include the case where the Poisson self-interaction potential influences the electrons dynamics too.

Submitted to: *J. Phys. A: Math. Gen.*

‡ Partially supported by Fundacao para Ciencia e Tecnologia, POCTI-ISFL-1-209 (Centro de Matematica e Applicacoes Fundamentais). Thanks are due to Dr. R. Carles for insightful comments.

1. Introduction

1.1. Preliminaries

It is a familiar fact that electrons are able to move over long distances inside certain materials; this phenomenon manifests itself, for instance, through the high electrical conductivity of metals. However, even in purest metals, electrons are influenced by the underlying lattice made of the atoms consituting the crystal itself. A very reasonable assumption is to consider the repartition of these atoms as periodic; such an idealization allows to take advantage of Bloch's theory which explains how valence/conduction electrons can move rather freely and have a well-defined (Bloch) momentum. Indeed, Bloch's theorem is one example of coherent electronic transport: in a perfect crystal at zero temperature, there is a great superposition of phase-coherent waves with similar wavenumbers which results in a frictionless flow inside the material (at low densities, Pauli's exclusion principle doesn't have very sensible effects). These electrons move according to the energy bands thus can survive multiple scattering events with the atoms without getting localized and accumulating somewhere. Unfortunately, finite conductivity is observed in practice because no sample will be pure enough to be a perfectly periodic lattice, and even if this idealization was realizable, vibrations due to thermal excitation would perturb the picture. The effects of these vibrations constitute the main point we want to study in this paper within a simplified framework.

We are interested in deriving approximate WKB solutions of certain Schrödinger equations in one space dimension, where short-range scattering effects other than those considered in the Bloch decomposition will be neglected. In other words, we shall work on ballistic transport of electrons for which the most important long-range interaction is the Coulomb force. In case one assumes translational invariance in two directions, three dimensional objects can be modelled to some extent by means of a one-dimesional mean-field equation. We shall follow these ideas which have already been studied in former works, [10, 11, 12]. However, we go now one step further considering that atoms vibrate as "coupled harmonic oscillators". The Hamiltonian for one electron reads (see [1], page 430), with obvious notation,

$$\mathcal{H}_{full} = \frac{p^2}{2m} + \sum_{\alpha\in\mathbb{Z}} \frac{P_\alpha^2}{2M} + \sum_{\alpha\in\mathbb{Z}} V_{ions}(|X_\alpha - X_{\alpha-1}|) + \sum_{\alpha\in\mathbb{Z}} V_{ion-e^-}(|x - X_\alpha|). \qquad (1)$$

Parameters (p, x, m) refer to some electron and $(P_\alpha, X_\alpha, M)_\alpha$ to the collection of atomic cores. One could also consider a cloud of electrons indexed by $\beta \in \mathbb{Z}$ and the first term in (1) should be replaced by

$$\sum_{\beta\in\mathbb{Z}} \frac{p_\beta^2}{2m} + \frac{1}{2} \sum_{\beta\neq\beta'} \frac{e^2}{|x_\beta - x_{\beta'}|}.$$

Then Coulomb self-interactions may be treated via "mean-field", which would lead to some Hartree equation, *cf.* [12]; this will be briefly considered in the numerical results of §4.3. But first, let us concentrate on the one-particle model (1). We shall assume the following hypotheses to hold throughout the whole paper:

- Ionic cores are coupled oscillators, *i.e.* $V_{ions}(|X_\alpha - X_{\alpha-1}|) = \frac{1}{2}M\omega^2(X_\alpha - X_{\alpha-1})^2$.
- They are treated classically (Born-Oppenheimer approximation) because $\frac{m}{M} \ll 1$.
- They influence electrons but not the opposite (there are no polarons, *cf.* [1, 19]).

1.2. Modelling of ionic cores vibrations

Without V_{ions}, ions would arrange periodically $\bar{X}_\alpha = 2\pi\alpha$, $\alpha \in \mathbb{Z}$, like in [10]; now, let's call $U_\alpha(t) := X_\alpha(t) - 2\pi\alpha$ the displacement around these abscissae "at rest". The cores' equation is decoupled thanks to our third hypothesis,

$$\frac{d}{dt^2}U_\alpha(t) - \omega^2\Big(U_{\alpha+1}(t) - 2U_\alpha(t) + U_{\alpha-1}(t)\Big) = 0.$$

As for the continuous wave equation, it can be solved by Fourier series:

$$Q(t,k) = \sum_{\alpha\in\mathbb{Z}} U_\alpha(t)\exp(-ik2\pi\alpha) \Rightarrow \frac{d}{dt^2}Q(t,k) = \Omega(k)^2 Q(t,k).$$

The dispersion relation reads, (see also [1])

$$\Omega(k) = 2\omega|\sin(k\pi)|, \qquad k \in \mathcal{B} := \Big]-\frac{1}{2},\frac{1}{2}\Big[,$$

with $\mathcal{B}$ the Brillouin zone associated to the Bravais lattice for the ionic cores "at rest". $U_\alpha(t)$ can be written as a continuous summation of plane waves:

$$U_\alpha(t) = \int_0^{\frac{1}{2}} A(k)\exp\Big(i(k2\pi\alpha - \Omega(k)t)\Big) + B(k)\exp\Big(-i(k2\pi\alpha - \Omega(k)t)\Big).dk. \quad (2)$$

The Schrödinger equation for the electron's wave function ψ becomes accordingly,

$$i\hbar\partial_t\psi + \frac{\hbar^2}{2m}\partial_{xx}\psi = V_{per}\Big(x + U_\alpha(\varepsilon t)\Big)\psi, \quad (3)$$

with $V_{per}(x) \simeq \sum_\alpha V_{ion-e^-}(|x - \bar{X}_\alpha|)$ can be considered 2π-periodic and smooth; the dimensionless paramenter $\varepsilon = \bar{T}_{e^-}/\bar{T}_{ions}$ is defined as the ratio of characteristic times for the movements of ions and electrons, respectively. This modelling has already been incontered in several papers; let us quote [20, 23] where it is referred to as "the deformed crystal". Moreover, many studies have been made in the field of "incommensurate crystals", see [16, 21, 18], emphasizing the so–called modulated Kronig-Penney model. This is somewhat an extreme case for which the potential showing up in (3) isn't periodic any more thus the Brillouin zone of the resulting crystal is reduced to a point. We believe that new methods are needed for tackling such a problem of non-periodic homogenization which goes beyond the scope of the present paper. Indeed all this text deals only with perturbed potentials (as showing up in the right-hand side of (3)) endowed with some perdiodicity.

2. WKB asymptotic expansions of wave functions

We assume the reader to be familiar with Bloch's theory; a comprehensive presentation is given in [1], see also [7, 8, 14, 15, 10]. In this section, we shall show that for simple enough displacements (2) (typically with few vibration modes), it is possible to derive a WKB approximation for the wave function ψ solution of (3) for smooth V_{per}. For simpliciy, we switch at once to "atomic units" for which $\hbar = m = e = 1$ and seek a convenient Ansatz as variables are rescaled according to $(t,x) \to (\varepsilon t, \varepsilon x)$ with $0 < \varepsilon \ll 1$; $\varepsilon = 0$ would mean that phonon scattering acts instantaneously.

2.1. Bloch theory and the Eikonal equation

We are now basically interested in the following equation:

$$i\varepsilon\partial_t\psi + \frac{\varepsilon^2}{2}\partial_{xx}\psi = \tilde{V}_{per}\left(t, \frac{x}{\varepsilon}\right)\psi, \qquad \tilde{V}_{per}(t,y) = V_{per}(y + u(t,y)), \tag{4}$$

where $y = x/\varepsilon$ is the microscopic variable, $\tilde{V}_{per}$ is supposed to be C^∞ in both variables, the motion u is smooth and periodic in both its variables, and V_{per} is 2π-periodic. The simplest case where u is only endowed with a unique vibration mode is displayed in Fig. 1. Let us assume that for all t, $\tilde{V}_{per}(t, y + 2\pi/k) = V_{per}(t,y)$; thus one can

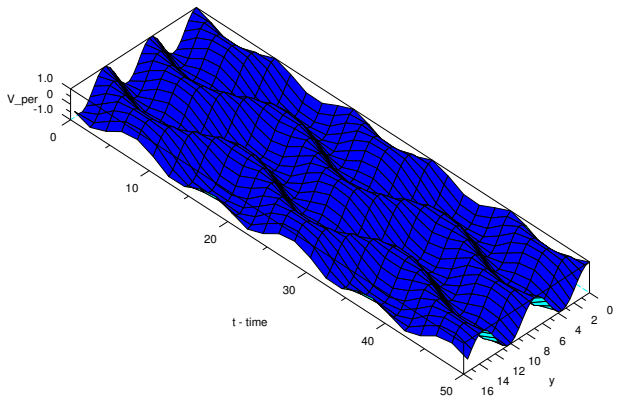

Figure 1. Time evolution for periodic potential in (4) with $V_{per}(y) = \cos(y)$ and $u(t,y) = \sin(ky + \Omega(k)t)$, $k \simeq 0.02$, $\varepsilon = 1$.

consider a slightly generalized Bloch eigenvalue problem:

$$\forall t \in \mathbb{R}, \qquad -\frac{1}{2}\partial_{yy}\Psi_{n,\kappa}(t,y) + \tilde{V}_{per}\left(t, \frac{x}{\varepsilon}\right)\Psi_{n,\kappa}(t,y) = E_n(t,\kappa)\Psi_{n,\kappa}(t,y), \tag{5}$$

for any $t \in \mathbb{R}^+$ and $\Psi_{n,\kappa}(t,y) = \exp(i\kappa y) z_{n,\kappa}(t,y)$ a Bloch state. We observe that we only need $y \in]0, 2\pi/k[$ and the Brillouin zone corresponding to $\tilde{V}_{per}$ is smaller than $\mathcal{B}$,

$$\kappa \in \tilde{\mathcal{B}} = \left]-\frac{k}{2}, \frac{k}{2}\right[, \qquad |k| \leq \frac{1}{2}.$$

Since there's no differentiation in time inside (5), standard results remain valid (see *e.g.* [17]) and ensure that for any fixed t and $\kappa \in \tilde{\mathcal{B}}$, there exists a complete set of eigenfunctions $\Psi_{n,\kappa}(t,.) \in L^2(0, 2\pi/k)$ with countably many eigenvalues $E_1(t,\kappa) < E_2(t,\kappa) < \cdots < E_{n-1}(t,\kappa) < E_n(t,\kappa) < \cdots$ depending smoothly on time. The set $\{E_n(t,\kappa); \kappa \in \tilde{\mathcal{B}}\}$ is called the n^{th} energy band whereas $\Psi_{n,\kappa}$ is a n^{th} Bloch state having the form $\exp(i\kappa y) z_{n,\kappa}(t,y)$ for a certain $2\pi/k$-periodic modulation. Modulations can be normalized so as to form an orthonormal base of $L^2(0, 2\pi/k)$ for each $t > 0$.

At this level, we introduce a WKB Ansatz for ψ considering a two-scale amplitude:

$$A\Big(t, x, y = \frac{x}{\varepsilon}\Big) = A_0(t,x,y) + \varepsilon A_1(t,x,y) + \cdots; \quad A\big(t, x, y + 2\pi/k\big) = A(t,x,y). \tag{6}$$

Plugging the approximation $A(t,x,x/\varepsilon)\exp(i\varphi(t,x)/\varepsilon)$ inside (4) and balancing the O(1) terms following carefully [7, 8, 14] can be shown to lead to an Hamilton-Jacobi equation for the phase:

$$\partial_t\varphi + E_n(t,\partial_x\varphi) = 0. \tag{7}$$

2.2. Derivation of the transport equation

The principal amplitude stems from balancing O(ε) terms and is usually handled by means of the "Feschbach method", see the paper [7] to which we refer for a detailed presentation of the computation. Here we shall limit ourselves to specify the changes occuring in the derivation because of the time-dependence of $\tilde{V}_{per}$. Actually, everything proceeds as in the Appendix A of [7], except for the last step that we explain now§: let us denote $\mathcal{L}$ the usual geometric optics transport operator associated to the Bloch theory:

$$\mathcal{L}a := E_n'(t,\partial_x\varphi)\partial_x a + \frac{1}{2}\partial_x(E_n'(t,\partial_x\varphi))a,$$

where E_n' stands for the partial derivative with respect to κ. The principal amplitude is defined as $a_0(t,x)$ such that there holds: $A_0(t,x,y) = a_0(t,x)z_{n,\kappa}(t,y)$ for $\kappa = \partial_x\varphi(t,x)$. From (A.4), (A.5), (A.6) in [7], we obtain the following equation for a_0:

$$\partial_t a_0 + a_0\int_0^{2\pi/k} g_n\overline{\partial_t g_n}.dy + E_n'(t,\partial_x\varphi)a_0\int_0^{2\pi/k} g_n\overline{\partial_x g_n}.dy + \mathcal{L}a_0 = 0, \tag{8}$$

where $g_n(t,x,y) = z_{n,\kappa=\partial_x\varphi(t,x)}(t,y)$. Now, as a consequence of the modulation's normalization, $\|z_{n,\kappa}(t,.)\|_{L^2(0,2\pi/k)} = 1$, we observe that the first coefficient acting on a_0 is purely imaginary,

$$\partial_t\int_0^{2\pi/k} g_n\overline{g_n}.dy = 0 = 2\Re\left(\int_0^{2\pi/k} g_n\overline{\partial_t g_n}.dy\right),$$

and since $E_n' \in \mathbb{R}$, the next one as well. It remains to make use of the definition of g_n, the chain rule, and the equation (7) to compute:

$$\int_0^{2\pi/k} g_n\left\{\overline{\partial_t g_n + E_n'(t,\partial_x\varphi)\partial_x g_n}\right\}.dy = \int_0^{2\pi/k} z_{n,\partial_x\varphi(t,x)}\,\overline{\partial_t z_{n,\kappa}}\big|_{\kappa=\partial_x\varphi(t,x)}.dy.$$

We denote this term $\beta(t,x) \in i\mathbb{R}$; it identifies with a Berry phase, [4], and stems from the time-dependence of the Bloch states. In case another slowly-varying potential $V(t,x)\psi$ was added on the right-hand side of (4), one would get another phase-shift too reading $\partial_x V(t,x)\int_0^{2\pi/k} z_{n,\partial_x\varphi(t,x)}\,\overline{\partial_\kappa z_{n,\kappa}}\big|_{\kappa=\partial_x\varphi(t,x)}.dy \in i\mathbb{R}$ like in [7, 8, 11]. Anyway, it now remains to multiply the resulting equation (8) by $\bar{a}_0$ and take its real part to derive the usual continuity equation for $|a_0|^2$:

$$\partial_t|a_0|^2 + \partial_x\Big(E_n'(t,\partial_x\varphi)|a_0|^2\Big) = 0. \tag{9}$$

All in all, we have shown that an approximate n^{th}-band solution for (4) reads

$$\psi^\varepsilon(t,x) = a_0(t,x)\exp\Big(i\varphi(t,x)/\varepsilon\Big)z_{n,\partial_x\varphi(t,x)}\Big(t,x/\varepsilon\Big), \qquad t \geq 0, \tag{10}$$

§ We shall use the same notations for easiness in reading.

and evolves in time according to the WKB system made of (7) and (9). A first consequence is that an initial datum concentrated on a given band will necessary give rise to an approximate solution in the same band. Lattice vibrations aren't supposed to make electrons trigger interband transitions; hence from now on, we consider some electron moving according to some energy band whose index $n \in \mathbb{N}$ is fixed.

2.3. "Lattice tracking" phenomenon

Clearly, each primitive cell of the "perturbed lattice" contains $\frac{1}{|k|} \in \mathbb{N}$ atomic cores. We modified the algorithm in [11], §2.2 in order to compute numerically $E_n(t,\kappa), \Psi_{n,\kappa}(t,y)$ by means of a spectral method. We write down:

$$\Psi_{n,\kappa}(t,y) = \sum_{\ell\in\mathbb{Z}} \hat{\Psi}^{\ell}_{n,\kappa}(t)\exp(i(n+\kappa)y/k),\ \hat{\Psi}^{\ell}_{n,\kappa}(t) = \int_0^{2\pi/k} z_{n,\kappa}(t,y)\frac{\exp(-iny/k)}{2\pi}.dy.$$

The same decomposition is carried out for the perturbed potential and one is led to diagonalize a matrix H_κ similar to that in [11] with kinetic energy terms reading now $\frac{k^2}{2}(\kappa+\ell)^2$, $\ell = -N, ..., N$. Modulations $z_{n,\kappa}$ are recovered by Fast Fourier transform (`fft`) of corresponding eigenvectors and there holds for some $t \in \mathbb{R}^+$, $n \in \mathbb{N}$:

$$E_n(t,\kappa) = \frac{\hat{E}_0(t)}{2} + \sum_{q\in\mathbb{N}^*} \hat{E}_q(t)\cos(2\pi q\kappa/k), \quad \hat{E}_q(t) = 4\int_0^{\frac{k}{2}} E_n(t,\kappa)\cos(2\pi q\kappa/k).d\kappa.$$

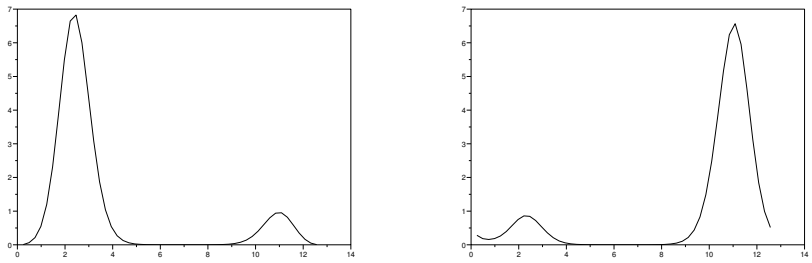

Figure 2. Two lowest modulations $|z_{n,\kappa=0}|^2$ for $k = 0.5$ and $t = 0.1$.

Since there are $1/k$ atoms per period, bands "stick together" and constitute sets of $1/k$ (for k small, there would be "bands of bands" emerging inside a tiny Brillouin zone). In the ground state, each of the $1/k$ modulations is very peaked around the corresponding atom in the elementary cell: see Fig. 2 where $\tilde{V}_{per}(t,y) = \cos\left(y + \frac{\pi}{2}\sin(ky + \Omega(k)t)\right)$. It is interesting to make a link with a feature pointed out in [23], namely the tendency for the lattice to drag the electron with its displacement motion, called "lattice tracking". First, observe that even if supplying the WKB system (7)–(9) with initial data such that $a_0 \equiv 1$ and $\partial_x\varphi \equiv 0$, we would have $\psi^\varepsilon(t,x) \neq \psi^\varepsilon(t=0,x)$ because of the time-dependence of $z_{n,\kappa}$. In other words, a small current is created from the motion of the atoms even if the macroscopic quantities remain constant in time. On Fig. 3, we displayed the deformations of the 5 lowest modulations with respect to the changes in the same potential $\tilde{V}_{per}$ as in Fig. 2. According to [10], §3.2, this implies the dragging effect suggested in [23].

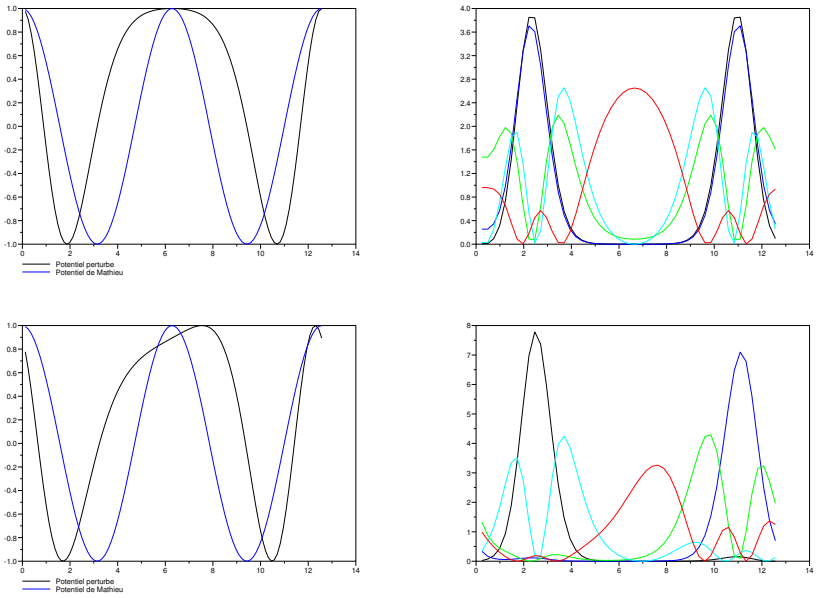

Figure 3. Potentials (left) and lowest modulations $|z_{n,\kappa=0}|^2$ (right) for $t = 0, 0.3$.

3. Numerical approximation with K-branch solutions

This method has been originally introduced in [9, 22] following the seminal work by Brenier and Corrias [6]. Is is based on the remark that geometrical solutions to (7)–(9) can be recovered from the solving of a rather simple system of nonlinear conservation laws through the moment closure of a kinetic equation. This opens the way of using all the results from the numerical analysis of this kind of problems instead of using the classical Lagrangian framework of ray-tracing algorithms, which may ask for repetitive regridding procedures. Let us also note that the inclusion of the Poisson self-consistent potential wouldn't be easy within a ray-tracing approach.

We don't plan to recall it completely instead we refer to [10, 11] where it has been explained how to extend it to the case where semi-classical dynamics are driven by energy bands obtained from Bloch's decomposition. The inclusion of the Poisson term for systems endowed with translational invariance in two directions has been described in [12] and will be used in §4.3. Here we just explain how to handle the time-dependence of the energy bands in the processing of the WKB system (7)–(9).

3.1. General procedure

It has been observed [5] that the geometric solutions of scalar conservation laws with a flux $E_n'(., u) \geq 0$ can be recovered out of a kinetic problem,

$$\partial_t f + E_n'(t, \xi)\partial_x f = 0, \qquad f(t = 0, x, \xi) = H(u(t = 0, x) - \xi)H(\xi),$$

with H the Heaviside function. Beyond breakup time, the form of f must express the fact that several particles with different velocities can cross at the same point x. Thus

a more correct representation would be,

$$f(t,x,\xi)=\sum_{j=1}^{K}(-1)^{j-1}H(u_j(t,x)-\xi), \tag{11}$$

as long as no more than K folds appear. A remarkable feature is that (11) can be obtained from an entropy minimization process; this eventually led to the definition of *K-multivalued solutions* in [6]:

Definition 1 *We call K-multivalued solution any measurable function* $f(t,x,\xi)\in\{0,1\}$ *on* $\mathbb{R}\times\mathbb{R}^+\times\mathbb{R}^+$ *satisfying the following equation in the sense of distributions*

$$\partial_t f+E_n'(t,\xi)\partial_x f=(-1)^{K-1}\partial_\xi^K\mu,\quad f(t,x,\xi)=\sum_{j=1}^{K}(-1)^{j-1}H(u_j(t,x)-\xi), \tag{12}$$

where μ *is a nonnegative Radon measure on* $\mathbb{R}\times\mathbb{R}^+\times\mathbb{R}^+$ *and* $K\in\mathbb{N}$ *is given.*

The set of $u_j(t,x)$'s is called the *K-branch entropy solution*; as usual, moments $m_i(t,x)=\frac{1}{i}\sum_{j=1}^{K}(-1)^{j-1}u_j(t,x)^{i-1}$, $i=1,2,...,K$ can be computed, for which an equivalence result holds:

Theorem 1 *(Brenier & Corrias, [6])*
A measurable function $f(t,x,\xi)=\sum_{j=1}^{K}(-1)^{j-1}H(u_j(t,x)-\xi)$ *is a K-multivalued solution if and only if all the following entropy inequalities hold for any* θ, $\partial_\xi^K\theta\geq 0$*:*

$$\partial_t\int_{\mathbb{R}^+}\theta(\xi)f(t,x,\xi).d\xi+\partial_x\int_{\mathbb{R}^+}E_n'(t,\xi)\theta(\xi)f(t,x,\xi).d\xi\leq 0. \tag{13}$$

Equality holds in case $\partial_\xi^K\theta\equiv 0$*, especially for* $\theta(\xi)=\xi^j$, $j=0,1,...,K-1$.

We close this section mentioning that the map $\mathbb{R}^K\ni\vec{m}\mapsto\vec{u}$ is called the "finite Markov moment problem"; this delicate inversion has been recently tackled in [13].

3.2. Moment systems and intensity recovery

Using `fft` routines in 2-D (t and κ or y), it is possible to obtain numerically good approximations of the following periodic functions, ($T_{per}<+\infty$)

$$[0,T_{per}]\times\tilde{\mathcal{B}}\ni t,\kappa\mapsto E_n(t,\kappa),$$

and,

$$[0,T_{per}]\times\left[0,\frac{2\pi}{k}\right]\times\tilde{\mathcal{B}}\ni t,y,\kappa\mapsto z_{n,\kappa}(t,y).$$

The fact that we restricted ourselves to commensurate crystals is fundamental here. These two representations wouldn't hold in Fourier space without assuming that $\tilde{V}_{per}$ is periodic in both its variables. This leads to restrictions on the k's allowed to show up in (2). If one introduces a velocity variable $u=\partial_x\varphi$ in (7), then a scalar conservation law with a time-dependent flux appears,

$$\partial_t u+\partial_x E_n(t,u)=0,\qquad u(t=0,.)=\partial_x\varphi(t=0,.),$$

for which the multivalued (or geometric) solution is to be sought according to the moment system (13). As soon as one completes this program, the principal intensity $|a_0|^2$ can be easily recovered; indeed, at any time $t > 0$, one deduces from (9) that

$$|a_0|^2(t,x) = |a_0|^2(t=0,x_0)\left|\frac{\partial x_0}{\partial x}\right|,$$

and from (7) that $x = x_0 + \int_0^t E_n'(s,u(t=0,x_0)).ds = x_0 + \int_0^t E_n'(s,u(t,x)).ds$ with $u(t,x)$ supposedly known from the solving of (13). In the homogeneous case, the most accurate way to derive the intensity follows from

$$\left|\frac{\partial x_0}{\partial x}\right| = \left|\frac{\partial x}{\partial x_0}\right|^{-1} = \left|\frac{1}{1+\partial_x u(t=0,x_0)\int_0^t E_n''(s,u(t,x)).ds}\right|,$$

which leads to the expression:

$$|a_0|^2(t,x) = \left|\frac{a_0(t=0,x_0)}{\sqrt{1+\partial_x u(t=0,x_0)\int_0^t E_n''(s,u(t,x)).ds}}\right|^2,\ x_0 = x - \int_0^t E_n'(s,u(t,x)).ds.$$

4. Numerical results

We now aim at showing results of K-branch solutions in the context of simple phonon scattering via the WKB approach (7)–(9) and to compare them to direct computations of solutions to (4) using the time-splitting Fourier schemes proposed in [2]. We shall try to show that the smaller ε, the closer the solutions' observables become. However, only weak convergence of observables can generally be hoped for [17], hence we shall look at the $L^1(\mathbb{R})$ norm of the antiderivative of the difference between position densities:

$$x \mapsto \int_0^x \left(\varrho^\varepsilon_{WKB}(T,s) - |\psi(T,s)|^2\right).ds, \qquad T \in \mathbb{R}^+. \tag{14}$$

This function can be expected to flatten as ε is decreased. $\varrho^\varepsilon_{WKB}$ stands for the position density obtained from the WKB ansatz (10). It's been sometimes necessary to filter numerically the Fourier schemes; here we used a standard convolution receipe involving a Gaussian kernel $\exp(-a\xi^2)$, $a \in \mathbb{R}^+$. 512 discretization points have been used for both algorithms.

4.1. One wavenumber

We first consider the perturbed potential which is 4π-periodic:

$$\tilde{V}_{per}(t,y) = \cos\left(y - \frac{\pi}{6}\sin(ky-t)\right), \qquad \omega = k = \frac{1}{2}. \tag{15}$$

The corresponding Brillouin zone is therefore $\tilde{\mathcal{B}} = [-\frac{1}{4},\frac{1}{4}]$ and Fig. 4 displays both the first conduction band and its associated modulation $|z_{n,\kappa=0}|^2$. The n index corresponds to the first conduction band, namely the first one with positive effective mass lying partially above the potential well. As time t goes by, the band is slightly deformed and not just translated. The initial data is of the form (10) with $\varphi(t=0,x) = \cos(x-\pi)/10$ and $|a_0|^2(t=0,x) = \exp(-(x-\pi)^2)/\pi$. We iterated up to

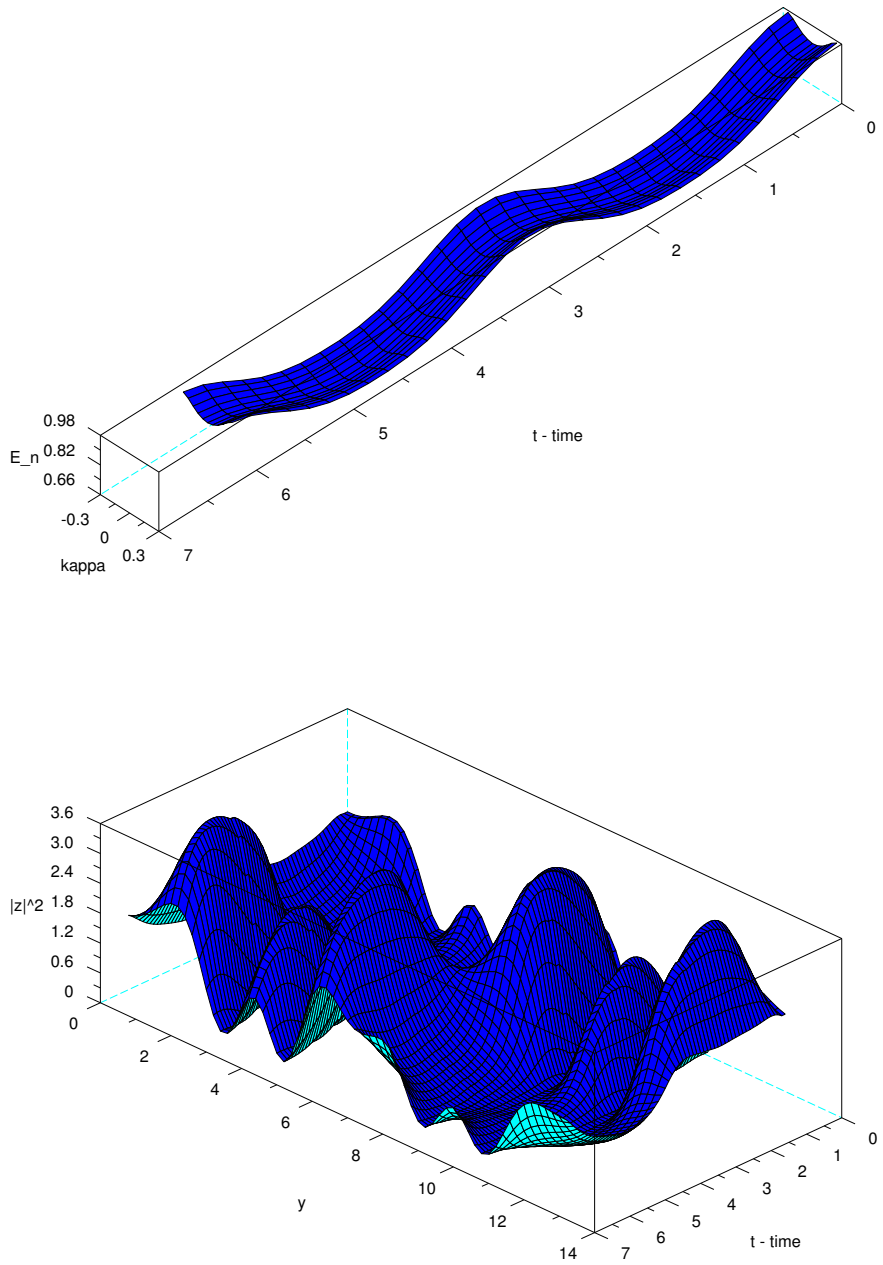

Figure 4. Time evolution of E_n (top) and $|z_{n,\kappa=0}|^2$ (bottom) for (15).

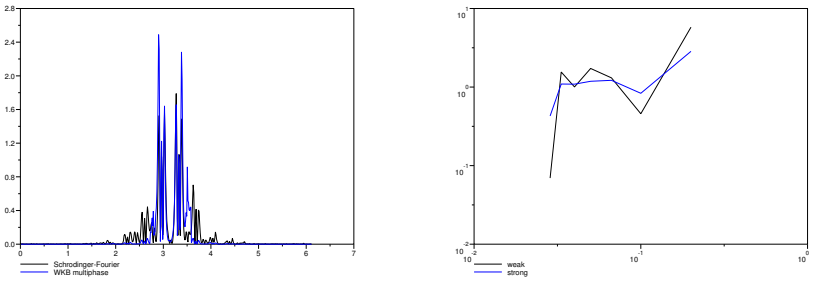

Figure 5. Position density for (15) in $T = 5$ and $\varepsilon = 1/35$ (left) and weak convergence as $\varepsilon \to 0$ ($L^1(\mathbb{R})$ norm of (14)).

$T = 5$ and the comparison between position densities is shown in Fig. 5 for $\varepsilon = 1/35$. The agreement is very satisfying and one even observes the weak convergence as ε decreases from $1/5$ to $1/35$ by checking the L^1 norm of (14). The following perturbed potential is still 4π-periodic, but slightly more involved,

$$\tilde{V}_{per}(t, y) = \cos\left(x - \frac{\pi}{6}\Big(0.7\sin(ky - t) + 0.3\cos(ky - t)\Big)\right), \tag{16}$$

where $\omega = k = \frac{1}{2}$. Results in $T = 5$ are shown in Fig. 6; once again, the agreement between both computations can be considered satisfying especially for $\varepsilon = 1/47$.

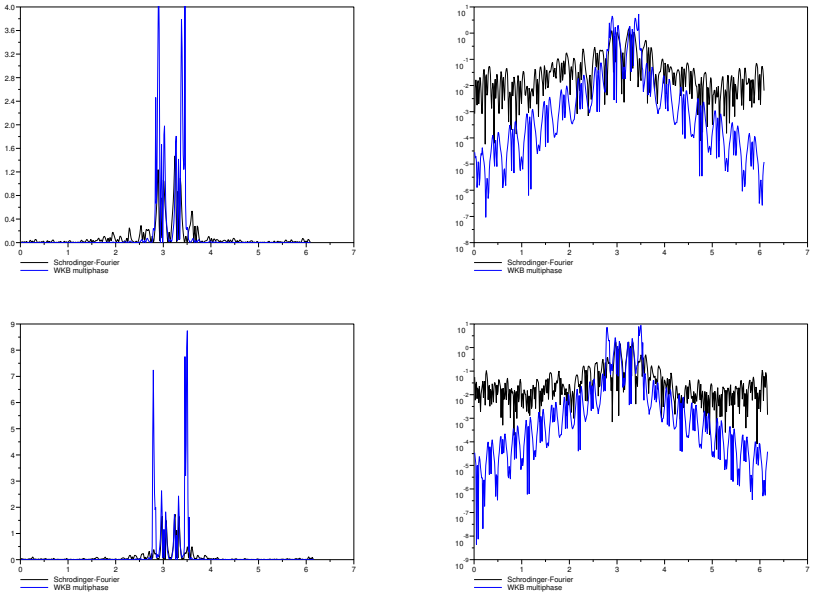

Figure 6. Position density for (16) in $T = 5$ and $\varepsilon = 1/35$ (top) and $\varepsilon = 1/47$ (bottom). Figures on the right are in log-scale.

4.2. Two different wavenumbers

We switch to the perturbed potential which is 12π-periodic:

$$\tilde{V}_{per}(t,y) = \cos\Big(x - \frac{\pi}{10}\Big(\sin(y/2-t) + \sin(y/6 - \Omega(1/6)t)\Big)\Big)\,. \tag{17}$$

This case is difficult because the Brillouin zone is very small ($k_1 = \frac{1}{6}$ and $k_2 = \frac{1}{2}$) thus (by smoothness) the bands are nearly flat and one must iterate for a long time to observe the dynamics. Fig. 7 displays the outcome in $T = 30$ of both WKB approach and direct Schrödinger computations from the initial data (10) with $\varphi(t=0,x) = \cos(x-\pi)/12$ and $|a_0|^2(t=0,x) = \exp(-(x-\pi)^2)/\pi$. We chosed the

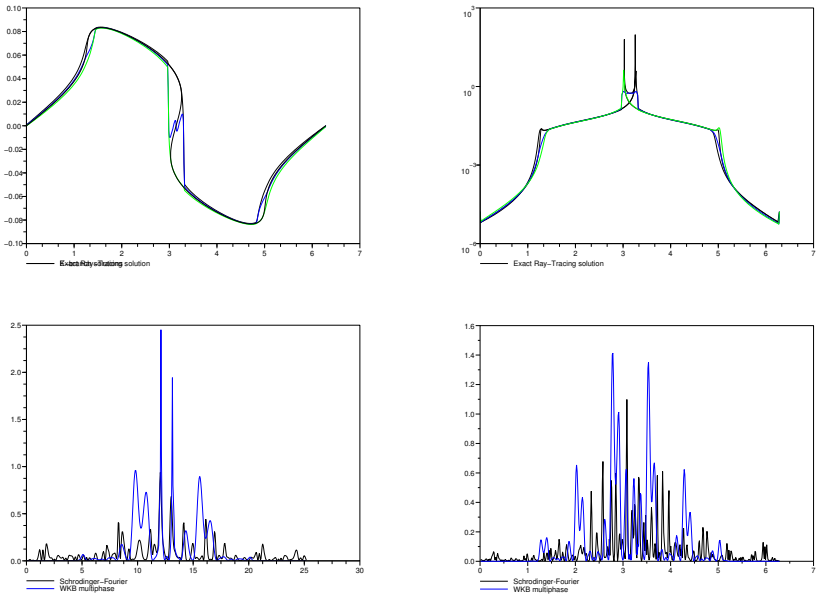

Figure 7. 3-branch velocity and intensity for (17) in $T = 30$ (top) and corresponding position density for $\varepsilon = 1/26$, $\varepsilon = 1/50$ (bottom).

two vibration modes $k = \frac{1}{2}$ and $k = \frac{1}{6}$ because the resulting $\tilde{V}_{per}$ is still a periodic function in y and t. Periodicity in t is important if one doesn't want to store all values of E_n involved in the computation. The agreement between position densities is less clear in this case, however the two central spikes are correctly located. 3-branch solutions are very good approximations of the ray-tracing picture, see again Fig. 7.

4.3. Inclusion of the Poisson potential

We move back to the simple perturbed potential (15) but we include now repulsive self-interaction effects between electrons. That is to say, we add a term $V_P(t,x)\psi$ on the right-hand side of (4), where $-\partial_{xx}V_P = |\psi|^2$. As a consequence, it hasn't been possible to obtain a breakup and multivalued K-branch solutions for $K > 1$. The perturbed potential and the initial data are the same than in §4.1 but iterations went only up to $T = 3$. It wasn't possible to display a ray-tracing solution in this

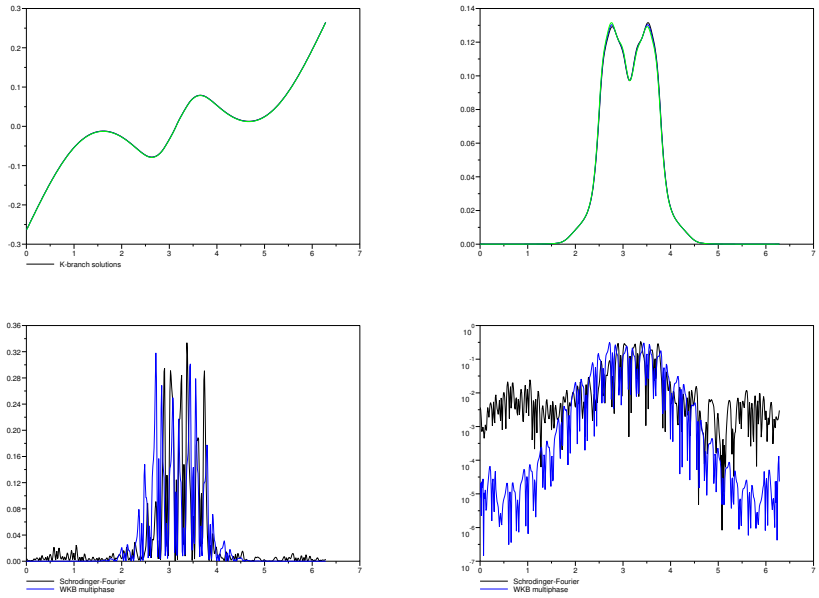

Figure 8. 3-branch velocity and intensity for (17) in $T = 3$ (top) and corresponding position density for $\varepsilon = 1/35$ (bottom).

weakly nonlinear case, thus we just observe a quite good adequation between position densities on Fig. 8. The $L^1(\mathbb{R})$ norm of (14) decreases slowly indeed with $\varepsilon \to 0$, as shown in Fig. 9, whereas strong L^1 convergence doesn't seem to be visible.

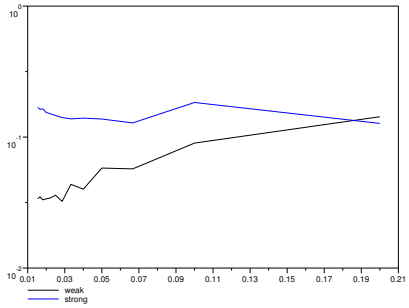

Figure 9. Decay of the $L^1(\mathbb{R})$ norm of (14) for $\varepsilon \in [1/65, 1/5]$.

5. Conclusion

We have proposed an original two-scale WKB technique adapted to electronic conduction in 1-D harmonic crystals, see (7)–(9)–(10). A numerical processing has been presented further together with a validation against direct Schrödinger computations. The main shortcoming in this general approach is that in case $\tilde{\mathcal{B}}$

becomes really tiny (that is to say, many small wave numbers are present in (2)), band gaps are likely to shrink so much as to allow electrons to perform interband transitions rather easily, thus a mixed state

$$\sum_{i=1}^{I} \lambda_i \psi^{\varepsilon}_{n_i}(t,x), \qquad \lambda_i \geq 0, \quad \sum_{i=1}^{I} \lambda_i = 1,$$

with $I = 1/k$ for instance, should be better considered (like in [3] for steady potentials) instead of the pure state (10). Still, our ansatz (10) is more precise compared to standard phonon modelling as a collision term in a kinetic equation. Indeed, one central hypothesis in this last approach is to assume that the resulting scattering effects are instantaneous; in other terms, $\varepsilon = 0$ and an adiabatic decoupling takes place. A major open problem lies in extending our analysis in §2 to non-periodic potentials, this would match the so–called incommensurate quasicrystals, [16, 21].

[1] N.W. Ashcroft and N.D. Mermin, Solid-state physics, Holt; Rinehart and Winston 1976.

[2] W.Z. Bao, Shi Jin and P.A. Markowich, *On time-splitting spectral approximations for the Schrödinger equation in the semiclassical regime*, J. Comp. Phys. **175** (2002), 487-524.

[3] P. Bechouche, N. Mauser, F. Poupaud, *Semiclassical limit for the Schrödinger-Poisson equation in a crystal*, Comm. Pure Applied Math. **54** (2001) 851–890.

[4] M. Berry, Proc. R. Soc. Lond. A **392**, 45 (1984)

[5] Y. Brenier, *Averaged multivalued solutions for scalar conservation laws*, SIAM J. Numer. Anal. **21** (1984), 1013 – 1037.

[6] Y. Brenier and L. Corrias, *A kinetic formulation for multibranch entropy solutions of scalar conservation laws*, Ann. I.H.P. Nonlinear Anal. **15** (1998), 169 – 190.

[7] R. Carles, P. Markowich, C. Sparber, *Semiclassical asymptotics for weakly nonlinear Bloch waves*, J. Stat. Phys. **117** (2004) 343–375.

[8] M. Dimassi, J.C. Guillot, J. Ralston, *Semiclassical asymptotics in magnetic Bloch bands*, J. Phys. A: Math. Gen. **35** (2002) 7597–7605.

[9] L. Gosse, *Using K-branch entropy solutions for multivalued geometric optics computations*, J. Comp. Phys. **180** (2002) 155–182.

[10] L. Gosse and P.A. Markowich, *Multiphase semiclassical approximation of an electron in a one-dimensional crystalline lattice – I. Homogeneous problems.*, J. Comp. Phys. **197** (2004) 387–417.

[11] L. Gosse, *Multiphase semiclassical approximation of an electron in a one-dimensional crystalline lattice – II. Impurities, confinement and Bloch oscillations.*, J. Comp. Phys. **201** (2004) 344–375.

[12] L. Gosse and N.J. Mauser, *Multiphase semiclassical approximation of an electron in a one-dimensional crystalline lattice – III. From ab-initio models to WKB for Schrödinger–Poisson.*, J. Comp. Phys. **211** (2006) 326–346.

[13] L. Gosse and O. Runborg, *Finite moment problems and applications to multiphase computations in geometric optics*, Comm. Math. Sci. **3** (2005) 373–392.

[14] J.C. Guillot, J. Ralston, E. Trubowitz, *Semiclassical asymptotics in solid-state physics*, Comm. Math. Phys. **116** (1988) 401–415.

[15] F. Hövermann, H. Spohn, S. Teufel, *Semiclassical limit for the Schrödinger equation for a short scale periodic potential*, Comm. Math. Phys. **215** (2001) 609–629.

[16] C. de Lange, T. Janssen, *Electrons in incommensurate crystals: spectrum and localization* Phys. Rev. B **28** (1983) 195–209.

[17] P. Markowich, N.J. Mauser, F. Poupaud, *A Wigner-function approach to semiclassical limits: electrons in a periodic potential*, J. Math. Phys. **35** (1994), 1066–1094.

[18] S. Mishra, S. Satpathy, *One-dimensional photonic crystal: the Kronig-Penney model* Phys. Rev. B **68** (2003) 045121.

[19] J. Nieto, *A generalized mean-field approach to the polaron*, Math. Models & Meth. Appl. Sci. **11** (2001) 1597–1607.

[20] Q. Niu, *Quantum adiabatic particle transport* Phys. Rev. B **34** (1986) 5093–5100.

[21] M. Quilichini, T. Janssen, *Phonon excitations in quasicrystals*, Rev. Mod. Phys. **69** (1997) 277–314.

[22] O. Runborg, *Some new results in multiphase geometrical optics*, Math. Mod. Numer. Anal. **34** (2000), 1203 – 1231.

[23] G. Sundaram, Q. Niu, *Wave-packet dynamics in slowly perturbed crystals: gradient corrections and Berry-phase effects*, Phys. Rev. B **59** (1999) 14915–14925.